

Ab-initio study of BaTiO₃ surfaces

J. Padilla and David Vanderbilt

Department of Physics and Astronomy, Rutgers University, Piscataway, NJ 08855-0849

(February 18, 1997)

We have carried out first-principles total-energy calculations of (001) surfaces of the tetragonal and cubic phases of BaTiO₃. Both BaO-terminated (type I) and TiO₂-terminated (type II) surfaces are considered, and the atomic configurations have been fully relaxed. We found no deep-gap surface states for any of the surfaces, in agreement with previous theoretical studies. However, the gap is reduced for the type-II surface, especially in the cubic phase. The surface relaxation energies are found to be substantial, i.e., many times larger than the bulk ferroelectric well depth. Nevertheless, the influence of the surface upon the ferroelectric order parameter is modest; we find only a small enhancement of the ferroelectricity near the surface.

I. INTRODUCTION

Recently there has been a surge of interest in the application of first-principles density-functional calculations to the study of the rich phenomenology of the perovskite oxides, with special attention to ferroelectric (FE) properties.¹ From these investigations, it has been found that the FE instability in these materials occurs as a result of a delicate balance between long-range Coulomb interactions that favor the FE state, and short-range forces that favor the cubic perovskite phase.^{2,3} Moreover, the ferroelectric properties are well known to degrade in thin-film⁴ and particulate⁵ geometries, suggesting that the FE state could be very sensitive to surface effects.

The cubic perovskites have the chemical formula ABO₃. For II-IV perovskites (e.g., BaTiO₃) A is a divalent cation and B is a tetravalent transition metal, while for I-V perovskites (e.g., KNbO₃) they are mono- and pentavalent respectively. The (001) and (111) surfaces of these materials have been most investigated experimentally.⁶ There are two possible terminations of the (001) surface: the AO-terminated surface (type-I) and the BO₂-terminated surface (type-II). In II-IV perovskites, the AO and BO₂ layers are charge-neutral, so that both type-I and type-II surfaces are non-polar. For I-V perovskites, the corresponding surfaces are instead polar. As for (111) surfaces, the atomic planes in this direction are of the form AO₃ and B, and are charged in either case, so that the (111) surfaces are polar. Since polar surfaces are expected to be relatively unstable, we have chosen to focus here on the (001) surfaces of a II-IV perovskite, BaTiO₃.

Due in part to the catalytic properties of SrTiO₃ and BaTiO₃,⁷ there has been a continuous interest in the surface properties of these materials. There have been previous theoretical studies especially for the case of the paraelectric SrTiO₃ surface, but also for BaTiO₃. Wolfram and coworkers⁸, using a linear combination of atomic orbitals (LCAO) cluster method, predicted mid-gap surface states for SrTiO₃, in disagreement with experimental

investigations.^{9,10} Only after *ad hoc* modifications to this model could the experimental results be accounted for.¹¹ Tsukada *et al.*¹² employed the DV X α cluster method to study SrTiO₃ surfaces, finding no mid-gap surface states. However, cluster methods are not very suitable for high-accuracy calculations of relaxations and electronic states on infinite surfaces, underlining the need for the application of more accurate, self-consistent techniques. While such techniques have recently yielded a great deal of insight into bulk perovskites,^{3,13-15} their application to the study of perovskite surfaces has not been very extensive. In fact, we only know of two such studies. Cohen^{16,17} presented linearized augmented plane wave (LAPW) calculations performed for slabs of tetragonal BaTiO₃ with (001) and (111) surfaces, using both symmetrical and asymmetrical terminations. Although some relaxations were allowed, the atomic positions were not fully relaxed. Kimura *et al.*¹⁸ used a plane-wave ultrasoft-pseudopotential¹⁹ approach (as in the present work) to study the TiO₂-terminated (001) surface of SrTiO₃, with and without oxygen vacancies at the surface. Again, the slabs were not fully relaxed.

In contrast, we study here symmetrically-terminated type-I and type-II surfaces of tetragonal and cubic BaTiO₃ (001) for which the coordinates have been fully relaxed by minimizing the total energy. This allows us to study the influence of surface relaxation effects upon the FE distortion. For the tetragonal phase, we consider only the case of the tetragonal *c* axis (i.e., polarization) parallel to the surface. (Polarization normal to the surface is suppressed by depolarization fields,³ at least for clean surfaces.) We employed the ultrasoft-pseudopotential method¹⁹ within the local-density approximation (LDA). This technique permits us to calculate the Hellmann-Feynman forces on each atom, making it possible to find the relaxed structure much more efficiently than for methods that compute only total energies.

Experimental studies of perovskite surfaces are complicated by the presence of surface defects,²⁰ making it

difficult to verify the surface stoichiometry. Therefore, most experimental investigations have not been very conclusive. On SrTiO_3 surfaces, the situation is better: the surface relaxations have been studied,²¹ and (as mentioned above) the absence of mid-gap surface state has been demonstrated.⁹ For BaTiO_3 surfaces, the experimental reports seem less conclusive. For example, evidence both for²² and against²³ surface gap states in this material have been published.

Regarding the degradation of FE properties for thin films and small particles as mentioned above,^{4,5} there does not seem to be any consensus about the origin of these effects. One possibility is that it is completely intrinsic, i.e., that the very presence of the surface suppresses the FE order in the vicinity of the surface. However, there are many other possible causes. These include the effects of surface-induced strain; perturbations of the chemical composition near the surface related to the presence of impurities, oxygen vacancies, or other defects; and the depolarization fields for the case of particles (or for films with polarization perpendicular to the surface). Here, we take a modest step in the direction of sorting out these effects by characterizing the purely intrinsic coupling between the presence of a surface and the FE order, for the case of a free (vacuum-terminated) surface. As we shall see, we find the surface relaxation energies are large compared to FE distortion energies. However, we find very little effect for type-I surfaces, and only a modest enhancement of the FE order at type-II surfaces, with indications that it will be mainly confined to just the first few atomic layers near the surface. Thus, it appears unlikely that intrinsic surface effects are responsible for the degradation of FE order in thin films and particles.

The remainder of the paper is divided as follows. In Sec. II, we describe the technical aspects of our first-principles calculations. In Sec. III, we report the results of our simulations. Finally, the main conclusions of the paper are reviewed in Sec. IV.

II. THEORETICAL DETAILS

We carried out self-consistent total-energy pseudopotential calculations in which the electronic wave functions were expanded in a plane-wave basis. The core electrons were frozen, and for a given geometry of the ions, the valence electron wavefunctions were obtained by minimizing the Kohn-Sham total-energy functional using a conjugate-gradient technique.²⁴ The exchange-correlation potential was treated with the LDA approximation in the Ceperley-Alder form.²⁵ The forces on each ion were relaxed to less than 0.02 eV/Å using a modified Broyden scheme.²⁶

The Vanderbilt ultrasoft pseudopotential scheme¹⁹ was employed. In this approach, the norm-conservation constraint is relaxed, allowing one to treat rather localized orbitals with a modest plane-wave cutoff. The pseu-

TABLE I. Computed and experimental values of structural parameters for BaTiO_3 in bulk cubic and tetragonal phases. a and c are lattice constants; δ_x are displacements associated with the FE instability as a fraction of c . O_I is the oxygen lying along \hat{x} from the Ti atom, and $\delta_x(\text{O}_\text{II}) = \delta_x(\text{O}_\text{III})$ by symmetry).

Phase	Parameter	Exper. ^a	Theory ^b
cubic	a (Å)	3.996	3.948
tetrag.	a (Å)	3.992	3.938
	c (Å)	4.036	3.993
	$\delta_x(\text{Ti})$	0.0135	0.0128
	$\delta_x(\text{O}_\text{I})$	-0.0150	-0.0150
	$\delta_x(\text{O}_\text{III})$	-0.0240	-0.0232

^aRef. 29.

^bRef. 24.

dopotentials for Ti, Ba and O are identical to those used previously²⁴ in a study of bulk perovskites. The semi-core Ti 3s and 3p states and Ba 5s and 5p states are included as valence levels. A plane-wave cutoff of 25 Ry has been used throughout; previous work has shown that the results are well-converged at this cutoff.

BaTiO_3 undergoes a series of phase transitions as the temperature is reduced, from the high-symmetry paraelectric cubic phase to FE phases with tetragonal, orthorhombic, and rhombohedral unit cells. The tetragonal structure is of special interest, since it is the room-temperature structure. In this paper, we are thus primarily interested in the surfaces of the room-temperature tetragonal phase, although for comparison we also present results for surface of the elevated-temperature cubic phase. Ideally one would like to do this by carrying out *ab-initio* molecular-dynamics simulations at the temperatures at which these phases are stable, but unfortunately this is not practical. Instead, we carry out ground-state ($T = 0$) calculations, but subject to the imposition of the appropriate (tetragonal or cubic) symmetry in order to prevent the system from adopting the true rhombohedral $T = 0$ structure. This is clearly an approximation, but we think it is a reasonable one. The computed ground-state structural parameters for the cubic and tetragonal bulk phases are given in Table I, together with experimental values for comparison. (Again, the theoretical values are for $T = 0$ structures with the appropriate symmetry imposed.) The computed lattice constants a and c for the cubic and tetragonal phases are 1 – 2% smaller than the experimental ones; this underestimation is typical of LDA calculations. We use the theoretical unit cell parameters in all calculations presented here.

As shown schematically in Fig. 1, the periodic slab corresponding to the type-I (BaO terminated) surface contains 17 atoms (4 BaO layers and 3 TiO_2 layers). Similarly, the type-II (TiO_2 terminated) slab contains 18 atoms (4 TiO_2 layers and 3 BaO layers). For both cases, the slabs were thus three lattice constants thick; the vac-

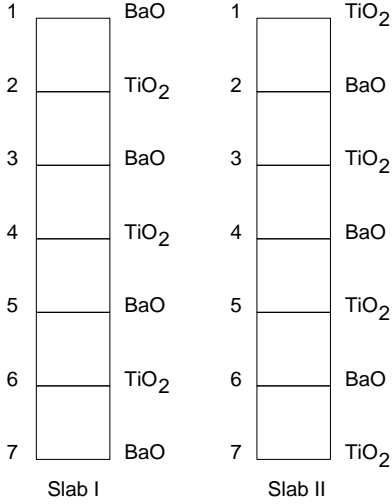


FIG. 1. Schematic arrangement of layers in the BaO-terminated (slab I) and TiO₂-terminated (slab II) supercell geometries. Layers 1 and 7 are surface layers.

uum region was two lattice constants thick. The z -axis is taken as normal to the surface, and the M_z mirror symmetry with respect to the central layer was imposed in all cases. For surfaces of the cubic phase, mirror symmetries M_x and M_y were also preserved. For the tetragonal case, the polarization vector and thus the tetragonal c -axis were chosen to lie along x (parallel to the surface); here, M_y symmetry was respected but m_x symmetry was allowed to be broken. As mentioned earlier, the choice of polarization parallel to the surface is motivated by the fact that no charge accumulation results at the surface for this case, and thus no depolarization fields appear.³ The case of the tetragonal c -axis lying perpendicular to the surface was considered by Cohen.^{16,17}

The calculations were done using a (4,4,2) Monkhorst-Pack mesh.²⁷ This corresponds to three and four k-points in the irreducible Brillouin zone (BZ) for the cubic and tetragonal supercells, respectively. To test the convergence with respect to k-point sampling, we repeated the calculation for a (6,6,2) mesh, finding that the surface energy differed by less than 3%. When the vacuum region was enlarged to three layers in thickness, the surface energy changed by less than 4%.

In order to study the relative stability of the two kinds of surface terminations, it is necessary to introduce appropriate chemical potentials.²⁸ To simplify our analysis, we think of the independent constituents of the slab as being BaO and TiO₂ units. We define E_f to be the *formation energy* needed to make bulk BaTiO₃ from BaO and TiO₂, per formula unit. Thus we have

$$-E_f = E_{\text{BaTiO}_3} - E_{\text{BaO}} - E_{\text{TiO}_2} \quad (1)$$

(by convention, $E_f > 0$). E_{BaTiO_3} , E_{BaO} , and E_{TiO_2} are the energies of the bulk crystals, per formula unit, measured relative to isolated ion cores and electrons. BaTiO₃ was calculated in the relaxed tetragonal structure, and

TABLE II. Atomic relaxations of the Ba-terminated surface (slab I) in the cubic (C) and tetragonal (T) phases, given as a fraction of a or c , with respect to ideal positions (i.e., for δ_x , with respect to the M_x symmetry plane).

Atom	δ_z (C)	δ_x (T)	δ_z (T)
Ba(1)	-0.0279	-0.0142	-0.0277
O _{III} (1)	-0.0140	-0.0298	-0.0126
Ti(2)	0.0092	-0.0086	0.0098
O _I (2)	0.0048	-0.0297	0.0059
O _{II} (2)	0.0048	-0.0240	0.0045
Ba(3)	-0.0053	-0.0149	-0.0059
O _{III} (3)	-0.0026	-0.0280	-0.0020
Ti(4)	0	-0.0034	0
O _I (4)	0	-0.0340	0
O _{II} (4)	0	-0.0256	0

TiO₂ in the relaxed rutile structure.

Now, we define the two chemical potentials μ_{TiO_2} and μ_{BaO} in such a way that $\mu_{\text{TiO}_2} = 0$ corresponds to a system in contact with a reservoir of bulk crystalline TiO₂, and similarly for μ_{BaO} . Furthermore, if we insist that the system is always in equilibrium with a reservoir of bulk BaTiO₃, then we have that

$$\mu_{\text{BaO}} + \mu_{\text{TiO}_2} = -E_f \quad (2)$$

Thus, only one of μ_{BaO} and μ_{TiO_2} is an independent degree of freedom. We arbitrarily chose μ_{TiO_2} as the independent one. Then μ_{TiO_2} can be allowed to vary over the range

$$-E_f \leq \mu_{\text{TiO}_2} \leq 0. \quad (3)$$

At $\mu_{\text{TiO}_2} = -E_f$ the system is in equilibrium with BaO and BaTiO₃, and for lower values bulk crystallites of BaO can precipitate. Similarly, above $\mu_{\text{TiO}_2} = 0$, bulk crystallites of TiO₂ can form.

Therefore, the grand thermodynamic potential per surface unit cell is given by

$$F = \frac{1}{2} [E_{\text{slab}} - N_{\text{TiO}_2}(\mu_{\text{TiO}_2} + E_{\text{TiO}_2}) - N_{\text{BaO}}(\mu_{\text{BaO}} + E_{\text{BaO}})] \quad (4)$$

(the factor of 1/2 appearing because the cell contains two surfaces), where E_{slab} is the energy of the relaxed slab in the tetragonal phase. For example, for the type-I slab, one has $N_{\text{TiO}_2} = 3$ and $N_{\text{BaO}} = 4$. Eqs. (2) and (4) give F as a function of μ_{TiO_2} over the range of Eq. (3).

III. RESULTS AND DISCUSSIONS

A. Structural relaxations

First we determined the equilibrium atomic positions for our two types of slabs in the two phases. For the

TABLE III. Atomic relaxations of the Ti-terminated surface (slab II) in the cubic (C) and tetragonal (T) phases, given as a fraction of a or c , with respect to ideal positions.

Atom	δ_z (C)	δ_x (T)	δ_z (T)
Ti(1)	-0.0389	0.0005	-0.0331
O _I (1)	-0.0163	-0.0499	-0.0100
O _{II} (1)	-0.0163	-0.0366	-0.0071
Ba(2)	0.0131	-0.0148	0.0186
O _{III} (2)	-0.0062	-0.0292	-0.0023
Ti(3)	-0.0075	0.0019	-0.0058
O _I (3)	-0.0035	-0.0372	-0.0022
O _{II} (3)	-0.0035	-0.0278	-0.0023
Ba(4)	0	-0.0111	0
O _{III} (4)	0	-0.0276	0

cubic surface, we started from the ideal structure and relaxed. For the tetragonal surface, we obtained a starting guess by superposing the z -displacements from the relaxed cubic surface with x -displacements from the bulk tetragonal structure.²⁴ The relaxed geometries are summarized in Tables II and III. In these tables, the atoms are listed in the same order as shown in Fig. 1. (Coordinates are only listed for atoms in the top half of the slab, $z \geq 0$; the others are determined by the M_z mirror symmetry.) By symmetry, there are no forces along \hat{x} or \hat{y} for the cubic surfaces, and no forces along \hat{y} for the tetragonal surface. Also due to the crystal termination, the two O atoms associated with the Ti atom (O_I and O_{II}), are no longer equivalent in the tetragonal phase (I, II, and III indicate the O that is connected to Ti by a bond along x , y , and z , respectively).

From Tables II and III, we can see that the largest relaxations are on the surface-layer atoms, as expected. They are especially important for the Ti atoms in the Ti-terminated slabs, in the direction perpendicular to the surface. This can plausibly be explained by noting that for bulk BaTiO₃, the filled Ba levels lie well below the oxygen-2 p valence-bands and do not hybridize strongly, so that the Ba atom is a relative spectator in the bonding.²⁴ In the tetragonal case, we can also see that the asymmetry between the two O atoms lying in a common surface plane is significant. Bond lengths on the surface change by less than 1.5% with respect to the bulk in the same phase (the latter values are the experimental ones, taken from Mitsui *et al.*²⁹).

We computed the average displacements β and the rumpling η for the surface layers; the results are given in Table IV. To fix notation, let $\delta z(M)$ be the change in the surface-layer metal-atom z position relative to the ideal unrelaxed structure, and $\delta z(O)$ be the same for the surface oxygens (defined as $[\delta z(O_I) + \delta z(O_{II})]/2$ for a TiO₂ layer). Then the surface relaxation parameter β is defined as $[\delta z(M) + \delta z(O)]/2$, and the rumpling η is defined as $[\delta z(O) - \delta z(M)]/2$. We find that the surface layers contract substantially inwards towards the bulk, with both

TABLE IV. Calculated interlayer relaxation (β) and rumpling (η) for the surface layer of the relaxed slabs in the cubic (C) and tetragonal (T) phases (Å).

Slab	β (C)	η (C)	β (T)	η (T)
Slab I	-0.08	0.03	-0.08	0.03
Slab II	-0.11	0.05	-0.08	0.05

the metal and oxygen ions relaxing in the same direction.

Cohen¹⁷ has computed the surface relaxations of an asymmetrically-terminated cubic slab (BaO on one surface and TiO₂ on the other). Detailed quantitative agreement is probably not expected, because (i) only the surface-layer atoms were relaxed in Cohen's calculation, and (ii) the asymmetric termination introduces a small electric field which may have influenced the relaxations. Nevertheless, we do find qualitative agreement. Cohen finds that the Ba and O atoms relax inwards by 0.043 and 0.033 lattice constants, respectively, on the Type-I surface; and the Ti and O atoms relax inwards by 0.048 and 0.027, respectively, on the type-II surface. These can be compared with the first two entries in the $\delta_z(C)$ column of Tables II and III. It can be seen that Cohen's values are 20-100% larger in magnitude, but of the same sign, as those that we calculate. Similarly, Cohen computes values of -0.15Å for the average surface layer relaxation, to be compared with the values given by us in the column $\beta(C)$ of Table IV. The rumpling computed by Cohen is also of the same sign, but different in detail, as that calculated by us.

We are not aware of any experimental surface structure determination for BaTiO₃ with which we can compare our theory. However, we note that a LEED I-V study of the corresponding SrTiO₃ surfaces²¹ comes to an opposite conclusion, suggesting an outward relaxation of the surface layer on the order of 0.1Å. While we have not carried out a parallel calculation on the SrTiO₃ surface, it appears unlikely that the mere replacement of Sr by the chemically similar Ba could be responsible for such a large qualitative discrepancy. Thus, we suggest that the experimental interpretation²¹ should be reexamined.

B. Influence of the surface upon ferroelectricity

It is important to understand whether the presence of the surface has a strong effect upon the near-surface ferroelectricity. For example, is the FE order enhanced near the surface, or is it suppressed? As we shall see in Sec. III C, the energy scale of the surface relaxations is larger than the energy scale of the FE double-well potential. Thus, a strong effect is possible. To analyze whether it really occurs, we computed an average FE distortion δ_{FE} for each layer of the slab. We define $\delta_{FE} = \delta_x(\text{Ba}) - \delta_x(\text{O}_{III})$ for a BaO plane, and $\delta_{FE} = \delta_x(\text{Ti}) - [\delta_x(\text{O}_I) + \delta_x(\text{O}_{II})]/2$ for a TiO₂ plane.

TABLE V. Calculated FE distortion δ_{FE} of the relaxed slabs, for each layer (units of lattice constant). Last line gives theoretical bulk values for reference.

Layer	Slab I		Slab II	
	$\delta_{\text{FE}}(\text{BaO})$	$\delta_{\text{FE}}(\text{TiO}_2)$	$\delta_{\text{FE}}(\text{BaO})$	$\delta_{\text{FE}}(\text{TiO}_2)$
1	0.0131			0.0345
2		0.0264	0.0165	
3	0.0157			0.0434
4		0.0259	0.0144	
Bulk	0.0232	0.0278	0.0232	0.0278

Our calculated values for δ_{FE} are given in Table V; the last row of the table gives the bulk values for reference. No clear pattern appears to emerge from these results, although we do note a moderate enhancement of the FE instability in the TiO_2 layers for the TiO_2 -terminated surface.

The lack of a clear trend for the influence of surface effects upon the FE distortion can be understood, at least in part, by noting that the FE mode is only one of three zone-center modes having the same symmetry.²⁴ The FE mode is distinguished as the one that is soft ($\omega^2 < 0$) in the cubic structure, but there is no particular reason why the surface relaxation should couple more strongly to this mode than to the others. We have estimated how strongly the surface relaxations are related to each of the zone-center modes by the following procedure. We calculate the forces for a tetragonal surface slab in which the displacements in the x direction are those of the ideal bulk tetragonal structure, while the displacements in the z direction are taken from the relaxed cubic surface. The forces in the x direction are then projected onto each of the zone-center bulk modes polarized along x . That is, the force for each type of atom (e.g., O_{III}) was summed over all such atoms in the slab, and the inner product was then taken between the resulting force vector and the bulk mode eigenvectors.

We found that the FE mode accounts for only about 31% and 26% of this force vector for the type-I and type-II slabs respectively. Thus, it seems that the distortions induced by the presence of the surface are mostly of non-FE character, helping to explain why the FE order is not as strongly affected as might have been guessed.

C. Surface energies

We turn now to a study of the surface energetics. Following the approach outlined in Sec. II, we calculated the grand thermodynamic potential F for our two types of surface as a function of TiO_2 chemical potential. The results are shown in Fig. 2. In order to attain optimal cancellation of errors, E_{TiO_2} and E_{BaO} were calculated within the LDA using the same pseudopotentials, and with the same 25 Ry energy cut-off. A similar k-point sampling

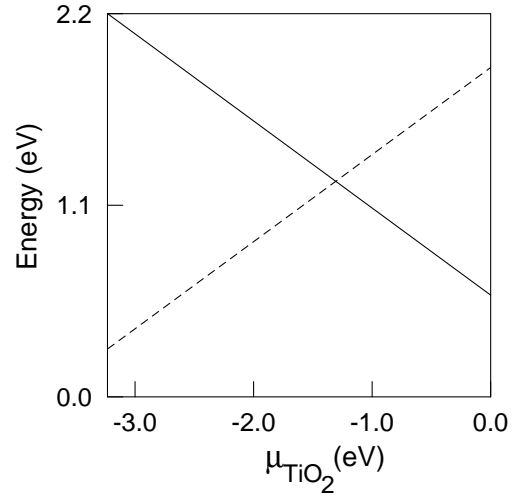


FIG. 2. Grand thermodynamic potential F as a function of the chemical potential μ_{TiO_2} , for the two types of surfaces, in the tetragonal phase. Dashed and solid lines correspond to type-I (BaO-terminated) and type-II (TiO_2 -terminated) surfaces respectively.

as for the surfaces of BaTiO_3 was also employed. In this way, we obtained $E_f = 3.23$ eV for the formation energy of BaTiO_3 . This quantity fixes the range of physical values of μ_{TiO_2} ; the left and right boundaries of Fig. 2 correspond to a system in thermodynamic contact with bulk BaO and bulk TiO_2 respectively. It can be seen that both surfaces have a comparable range of thermodynamic stability, indicating that either type-I or type-II surfaces could be formed depending on whether growth occurs in Ba-rich or Ti-rich conditions.

The *average* surface energy E_{surf} (i.e., the average of F for the two kind of surfaces) is independent of μ_{TiO_2} . Therefore, this quantity is suitable for comparisons. For the cubic phase, we estimated E_{surf} for the (001) surfaces to be 1.241 eV per surface unit cell (1265 erg/cm²); and for the tetragonal phase, it was estimated to be 1.237 eV per surface unit cell (1260 erg/cm²). The value of the average E_{surf} calculated in Ref. 17 for the symmetrically-terminated cubic (001) surfaces is 920 erg/cm². As pointed out in that paper, the large value of E_{surf} may help explain why BaTiO_3 does not cleave easily, but fractures instead.

In order to compute the surface relaxation energy E_{relax} , we computed the average surface energy E_{unrel} for the *unrelaxed* cubic slabs (i.e., atoms in the ideal cubic perovskite positions), using the same k-point sampling as for the relaxed systems. We obtained $E_{\text{unrel}} = 1.358$ eV. Thus, the relaxations account for 0.127 eV of the surface energy per surface unit cell (or about 130 erg/cm²).

Note that E_{relax} is many times larger than the bulk ferroelectric well depth, estimated to be of the order of 0.03 eV. This would indicate that the surface is capable of acting as a strong perturbation on the FE order. As explained in Sec. IIIB, however, the actual effect is

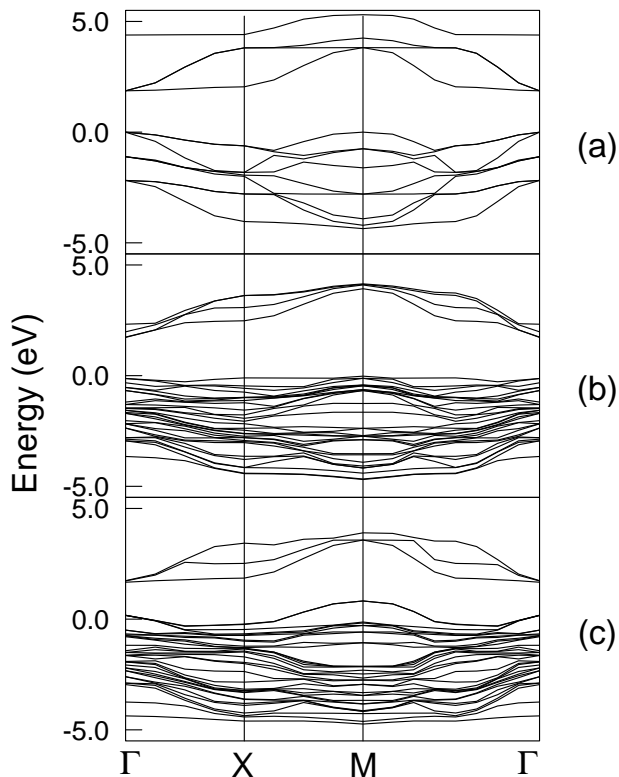


FIG. 3. Calculated band structures for BaTiO_3 in the cubic phase. (a) Surface-projected bulk band structure. (b) BaO-terminated surface (slab I). (c) TiO_2 -terminated surface (slab II). The zero of energy corresponds to the bulk valence band maximum. Only the lowest few conduction bands are shown.

more modest than one would guess based on energetic considerations alone.

D. Surface band structure

We have carried out LDA calculations of the surface electronic structure for our various surface slabs. While the LDA is well known to be quantitatively unreliable as regards excitation properties such as band gaps, we believe that the results presented here are nevertheless likely to be qualitatively correct. The bulk band gap in our calculation is 1.8 eV, to be compared with the experimental value of 3.2 eV; this level of disagreement is typical for the LDA.

Fig. 3 shows the calculated LDA band structure for cubic bulk BaTiO_3 projected onto the surface BZ, and the surface band structures for the Ba- and Ti-terminated relaxed surfaces in the cubic phase. (The zero of energy for each surface slab was established by aligning the Ba or Ti semicore s states in the interior layers of the slab with those of the bulk.) Plots for the tetragonal surfaces would look similar, except that the tendency for states to intrude into the gap is stronger for the cubic case. This

TABLE VI. Calculated band gaps for relaxed cubic (C) and tetragonal (T) surface slabs (eV).

Slab	C	T
Slab I	1.80	2.01
Slab II	0.84	1.18
Bulk	1.79	1.80

can be seen in Table VI, where we list the calculated band gaps for both cubic and tetragonal slabs. We therefore tend to focus on the cubic surfaces, where it is easier to identify and characterize the surface states.

First, we can see that on the Ba-terminated (type-I) surface, the gap is not reduced and there are no deep gap states. On the Ti-terminated (type-II) surface, however, the gap is reduced, especially for the cubic case. As can be seen from Fig. 3(c), there is a tendency for valence-band states to intrude upwards into the lower part of the band gap for this surface, especially near the M point of the surface BZ. (Qualitatively similar results can be seen in Fig. 3 of Ref. 17.) However, the conduction band does not change much with respect to the bulk. Moreover, we do not see signs of any true “deep-gap” states lying near the center of the gap. As noted earlier, the existence of such deep-gap states remains controversial experimentally. Our work suggests that if gap states do exist in connection with non-defective (001) surfaces, it is likely that they would be found in the lower part of the band gap, and that this would be indicative of exposed TiO_2 (as opposed to BaO) surface planes.

Figure 4 illustrates the character of the valence-band state at the M point that is intruding into the lower part of the gap. The total charge density is also shown for reference. It can be seen that this state is composed of O $2p$ lone-pair orbitals lying in the surface plane. Further inspection shows that the special feature of this state is that the wavefunction has four nodal planes [(100), (110), (010), and $(\bar{1}10)$] intersecting at the Ti sites. This precludes the presence of any Ti $3d$ character (in fact, any Ti character of angular momentum $l < 4$). In the bulk, the oxygen $2p$ orbitals are all hybridized with Ti $3d$ orbitals to some extent, and the level repulsion associated with this hybridization pushes the energy location of the valence-band states downward in energy. Thus, the energy of the unhybridized O $2p$ lone-pair surface state at the M point is left intruding into the lower part of the gap.

This insight makes it possible to understand other features of the surface band structures as well. For example, on the BaO-terminated surface, every surface oxygen atom is directly above a Ti atom, and is strongly hybridized to it. Thus, there is no such tendency for the formation of surface states in this case. Returning to the TiO_2 -terminated surface, there seems to be a weaker tendency for the intrusion of a valence-band derived surface state at Γ . This state turns out to have a single nodal

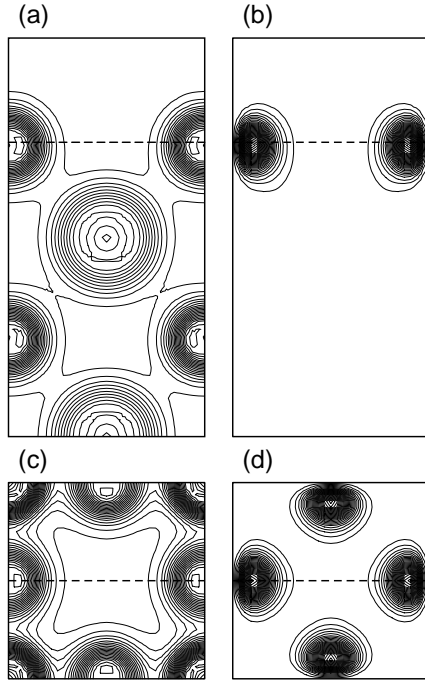


FIG. 4. Charge-density plots for relaxed Ti-terminated surface (slab II) in the cubic phase. Panels (a-b) show cuts on a vertical x - z BaO plane; panels (c-d) show cuts on the x - y surface TiO_2 plane. Total charge density, (a) and (c); charge density of highest occupied state at M point of the surface BZ, (b) and (d).

plane passing through the Ti site, so that hybridization with Ti 3d orbitals is only weakly allowed (by the breaking of M_z mirror symmetry across the surface plane).

We expect that these results would remain qualitatively valid for other II-VI perovskites such as SrTiO_3 or PbZrO_3 . For I-V perovskites such as KNbO_3 and LiTaO_3 , however, the (001) surface is non-stoichiometric, and the surface electronic structure would be expected to be quite different.

IV. SUMMARY

In summary, we have carried out LDA density-functional calculations of BaO- and TiO_2 -terminated (001) surfaces for cubic and tetragonal phases of BaTiO_3 . By minimizing the forces on the ions, we obtained the relaxed ionic structures. As would have been expected from the bulk electronic levels of BaTiO_3 , the most important relaxations occur for the TiO_2 -terminated surfaces. There appears to be a modest tendency for the surface relaxations to enhance the FE distortion on that surface, although the situation is complicated by the fact that the relaxations excite modes other than the soft zone-center one.

The free energies for the different surfaces were calculated as a function of the TiO_2 chemical potential.

In particular, the average surface energy was found to be about 1260 erg/cm^2 . The surface relaxation energies were found to be around 10% of the total surface energy.

In accord with previous theoretical reports, no mid-gap surface levels are found. But for the TiO_2 terminated surfaces, there is a substantial reduction of the bulk gap, especially for the cubic-phase surface. This reduction results from the intrusion of states of valence-band character into the lower part of the band gap, especially near the M point of the surface BZ.

ACKNOWLEDGMENTS

This work was supported by the ONR grant N00014-91-J-1184 and NSF grant DMR-91-15342. We also acknowledge Cray C90 computer time provided by the Pittsburgh Supercomputing Center under grant DMR930042P.

- ¹ M.E. Lines and A.M. Glass, *Principles and Applications of Ferroelectrics and Related Materials*, (Clarendon Press, Oxford, 1977); F. Jona and G. Shirane, *Ferroelectric Crystals*, (Dover Publications, New York, 1993).
- ² R. Resta, M. Posternak, and A. Baldereschi, *Phys. Rev. Lett.* **70**, 1010 (1993).
- ³ W. Zhong, R. D. King-Smith and D. Vanderbilt, *Phys. Rev. Lett.* **72**, 3618 (1994).
- ⁴ F. Tsai and J.M. Cowley, *Appl. Phys. Lett.*, **65**, 1906 (1994).
- ⁵ J.C. Niepce, *Surface and Interfaces of Ceramic Materials*, edited by L.C. Dufour (Kluwer Academic Publishers, 1989), p. 521.
- ⁶ V.E. Henrich and P.A. Cox, *The Surface Science of Metal Oxides*, (Cambridge University Press, New York, 1994).
- ⁷ M. Tomkiewicz and H. Fay, *Appl. Phys.*, **18**, 1 (1979).
- ⁸ T. Wolfram, E.A. Kraut, and F.J. Morin, *Phys. Rev. B* **7**, 1677 (1973).
- ⁹ R.A. Powell and W.F. Spicer, *Phys. Rev. B* **13**, 2601 (1976).
- ¹⁰ V.E. Henrich, G. Dresselhaus, and H.J. Zeiger, *Bull. Am. Phys. Soc. Ser. II* **22**, 364 (1977).
- ¹¹ S. Ellialtioglu, T. Wolfram, and V.E. Henrich, *Solid State Commun.* **27**, 321 (1978).
- ¹² M. Tsukada, C. Satoko, and H. Adachi, *J. Phys. Soc. Jpn.* **48**, 200 (1980).
- ¹³ W. Zhong, D. Vanderbilt, and K.M. Rabe, *Phys. Rev. Lett.* **73**, 1861 (1994); *Phys. Rev. B* **52**, 6301 (1995).
- ¹⁴ R.E. Cohen and H. Krakauer, *Phys. Rev. B* **42**, 6416 (1990); R.E. Cohen and H. Krakauer, *Ferroelectrics* **136**, 65 (1992); R.E. Cohen, *Nature* **358**, 136 (1992).
- ¹⁵ D.J. Singh, *Ferroelectrics* **164**, 143 (1995).
- ¹⁶ R.E. Cohen, *J. Phys. Chem. Solids* **57**, 1393 (1996).
- ¹⁷ R.E. Cohen, *Ferroelectrics*, in press.

- ¹⁸ S. Kimura *et al.*, Phys. Rev. B **51**, 11049 (1995).
- ¹⁹ D. Vanderbilt, Phys. Rev. B **41**, 7892 (1990).
- ²⁰ B. Cord and R. Courths, Surface Science, **152/153**, 1141 (1985).
- ²¹ T. Hikita, T. Hanada and M. Kudo, Surface Science, **287/288**, 377 (1993).
- ²² S. Robey, Ferroelectrics, *in press*, (1996).
- ²³ S.M. Mukhopadhyay and T.C.S. Chen, J. Mat. Res. **10**, 1502 (1995).
- ²⁴ R.D. King-Smith and D. Vanderbilt, Phys. Rev. B **49**, 5828 (1994).
- ²⁵ D.M. Ceperley and B.J. Alder, Phys. Rev. Lett. **45**, 566 (1980).
- ²⁶ D. Vanderbilt and S.G. Louie, Phys. Rev. B **30**, 6118 (1984).
- ²⁷ H.J. Monkhorst and J.D. Pack, Phys. Rev. B **13**, 5188 (1976).
- ²⁸ G.-X. Qian, R.M. Martin and D.J. Chadi, Phys. Rev. B **38**, 7649 (1988).
- ²⁹ T. Mitsui *et al.*, *Landolt-Bornstein numerical data and functional relationships in science and technology* (Springer-Verlag,1981), NS, III/**16**.